ESTIMATES OF THE CLIMATE RESPONSE TO AIRCRAFT CO_2 AND NO_X EMISSIONS SCENARIOS

ROBERT SAUSEN and ULRICH SCHUMANN
Deutsches Zentrum für Luft- und Raumfahrt, Institut für Physik der Atmosphäre, Oberpfaffenhofen, D-82234 Weßling, Germany

Abstract. A combination of linear response models is used to estimate the transient changes in the global means of carbon dioxide (CO_2) concentration, surface temperature, and sea level due to aviation. Apart from CO_2, the forcing caused by ozone (O_3) changes due to nitrogen oxide (NO_x) emissions from aircraft is also considered. The model is applied to aviation using several CO_2 emissions scenarios, based on reported fuel consumption in the past and scenarios for the future, and corresponding NO_x emissions.

Aviation CO_2 emissions from the past until 1995 enlarged the atmospheric CO_2 concentration by 1.4 ppmv (1.7% of the anthropogenic CO_2 increase since 1800). By 1995, the global mean surface temperature had increased by about 0.004 K, and the sea level had risen by 0.045 cm.

In one scenario (*Fa1*), which assumes a threefold increase in aviation fuel consumption until 2050 and an annual increase rate of 1% thereafter until 2100, the model predicts a CO_2 concentration change of 13 ppmv by 2100, causing temperature increases of 0.01, 0.025, 0.05 K and sea level increases of 0.1, 0.3, and 0.5 cm in the years 2015, 2050, and 2100, respectively. For other recently published scenarios, the results range from 5 to 17 ppmv for CO_2 concentration increase in the year 2050, and 0.02 to 0.05 K for temperature increase.

Under the assumption that present-day aircraft-induced O_3 changes cause an equilibrium surface warming of 0.05 K, the transient responses amount to 0.03 K in surface temperature for scenario *Fa1* in 1995. The radiative forcing due to an aircraft-induced O_3 increase causes a larger temperature change than aircraft CO_2 forcing. Also, climate reacts more promptly to changes in O_3 than to changes in CO_2 emissions from aviation. Finally, even under the assumption of a rather small equilibrium temperature change from aircraft-induced O_3 (0.01 K for the 1992 NO_x emissions), a proposed new combustor technology which reduces specific NO_x emissions will cause a smaller temperature change during the next century than the standard technology does, despite a slightly enhanced fuel consumption. Regional effects are not considered here, but may be larger than the global mean responses.

1. Introduction

Aircraft emissions can modify the climate in several ways: (1) aircraft emit substances which are radiatively active (e.g., CO_2); (2) they emit substances which produce or destroy radiatively active substances (e.g., NO_x which modifies O_3 concentration); (3) emissions trigger the generation of additional clouds (e.g., contrails).

The most reliable results on the effects of aircraft emissions are expected from simulations with a comprehensive atmosphere-ocean general circulation model

Climatic Change **44:** 27–58, 2000.

(GCM) or with an atmosphere GCM coupled to a model of the oceanic mixed layer. These models have to be complemented by models of the carbon cycle and models of atmospheric chemistry. Such models have been used in various studies to assess the climate change due to the anthropogenic increase in greenhouse gases and sulphate aerosols (e.g., IPCC, 1996). However, only a rather limited number of GCM studies on aircraft climate effects exist (e.g., Rind and Lonergan, 1995; Ponater et al., 1996; Rind et al., 1996; Sausen et al., 1997). Currently, no GCM study is available that comprises all potential aircraft effects (see Schumann (1997) and Brasseur et al. (1998), for overviews on aircraft effects on the climate). Furthermore, such studies are very expensive in computational resources, which limits the number of potential simulations.

In order to provide estimates of the climatic impact (in terms of global mean surface temperature and sea level change) of several scenarios of aircraft emissions, we use linear response models, which have previously been tuned to reproduce certain aspects of a comprehensive climate model or a carbon cycle model, respectively. Such models were used to study the cold start effect, for instance (Hasselmann et al., 1993). Simplified models of a somewhat different type were applied to explore the impact of various IPCC (1992) emissions scenarios (Enting et al., 1994; IPCC, 1996).

In this study, we will concentrate on changes in CO_2 concentrations as they arise from several aircraft emissions scenarios of CO_2. The impact of NO_x emissions on O_3 and the resulting climate changes are considered in a simplified manner without simulating the details of atmospheric chemistry. Instead, we assume that the relation between NO_x emissions and the resulting equilibrium climate response is known. The effects of other emissions and potential cloud cover changes are not considered in this study. We diagnose the radiative forcing and give estimates of the changes in the global mean surface temperature and in the global mean sea level. We will compare our results with previous estimates, as reported in Friedl (1997) and Brasseur et al. (1998). Finally, we will discuss the difference between the responses from transient and equilibrium simulations, and the trade-off from different technology options of combustor development.

2. Models

If we consider small perturbations of the climate system about an equilibrium reference state, we can describe the response of the climate system to perturbing forcings in terms of a linear response model. Here, the response of a climate variable $\Phi(t)$ (where t is time) to a forcing $F(t)$ (with $F(t) = 0$ for $t < t_0$) is described by a convolution integral,

$$\Phi(t) = \int_{t_0}^{t} G_\Phi(t - t')\, F(t')\, dt'. \tag{1}$$

$G_\Phi(t)$ is the impulse response (Green) function, which describes the response to a 'δ'-forcing at $t = 0$. Both $F(t)$ and $\Phi(t)$ are perturbations relative to an equilibrium reference state (see Hasselmann et al. (1993), for further details).

In our case, forcing will be either the CO_2 emissions rate or the CO_2 concentration. The responding climate variable will be the CO_2 concentration or the global mean surface temperature and sea level changes, respectively. Aircraft NO_x emissions will also be considered as forcing.

The impulse response function is characteristic for the climate system and the regarded equilibrium reference state. It can be determined from simulations with a carbon cycle model or a comprehensive climate model. For any non-degenerate linear system, the response can be represented as a linear superposition of the response of individual modes with complex eigenvalues, $\mu_j = \lambda_j - i\omega_j$,

$$G_\Phi(t) = \sum_j \alpha_j \, \mathrm{e}^{-\mu_j t}. \tag{2}$$

Real eigenvalues ($\omega_j = 0$) occur singly, whereas complex eigenvalues ($\omega_j \neq 0$) occur in complex conjugate pairs (Hasselmann et al., 1993).

We will use the impulse response function in the form of (2). The coefficients are fixed by demanding that (2) approximates results from simulations with a carbon cycle model or a comprehensive climate model, respectively. In our case, only real eigenvalues occur. We can then transform (2) to

$$G_\Phi(t) = \sum_j \alpha_j \, \mathrm{e}^{-t/\tau_j}, \tag{3}$$

where τ_j is the e-folding time of mode j. The equilibrium response of mode j to a unit forcing is $\alpha_j \, \tau_j$.

The response of the CO_2 concentration $C(t)$ to CO_2 emissions rate $E(t)$ is modeled as in Hasselmann et al. (1997), approximating the results of the carbon cycle model of Meier-Reimer and Hasselmann (1987),

$$\Delta C(t) = \int_{t_0}^{t} G_C(t - t') \, E(t') \, dt', \tag{4}$$

and

$$G_C(t) = \sum_{j=0}^{5} \alpha_j \, \mathrm{e}^{-t/\tau_j}, \tag{5}$$

with the parameters of Table I.

The radiative forcing of the well-mixed greenhouse gas CO_2 is roughly proportional to the logarithm of the concentration. The logarithmic function approximates the saturation in radiative forcing with increasing CO_2 concentration. As a consequence, an additional CO_2 amount has a smaller effect at higher background CO_2 concentration (IPCC, 1992).

TABLE I
Coefficients of the impulse response function G_C for the CO_2 concentration

j	1	2	3	4	5
α_j [ppbv/Tg(C)]	0.067	0.1135	0.152	0.0970	0.041
τ_j [yr]	∞	313.8	79.8	18.8	1.7

Following Hasselmann et al. (1993), we calculate a (normalized) radiative forcing RF^* due to CO_2 changes

$$RF^*(t) = \frac{\ln(C(t)/C_0)}{\ln 2}\,, \tag{6}$$

where C_0 is the observed CO_2 concentration at the preindustrial time $t_0 = 1800$ yr. RF^* is normalized such that $RF^* = 1$ for a CO_2 doubling.

The radiative forcing in units of Wm^{-2} can be estimated from the normalized forcing (6) as

$$RF(t) = \frac{RF^*(t)}{RF_T^*(1992)} \times 1.56\ \mathrm{Wm}^{-2}\,, \tag{7}$$

assuming that the CO_2 increase from 1800 until 1992 caused a total radiative forcing of 1.56 Wm^{-2} (IPCC, 1995). $RF_T^*(1992)$ is the respective total normalized radiative forcing due to CO_2. The values of $RF(t)$ will only be used for diagnostics.

The global mean surface temperature ΔT and sea level Δh responses are computed using only one (exponentially decaying) mode in (5), as derived in Hasselmann et al. (1993, 1997), by approximating results from an atmosphere-ocean GCM simulation for the IPCC scenario A (Cubasch et al., 1992):

$$\Delta T(t) = \int_{t_0}^{t} G_T(t-t')\, RF^*(t')\, dt'\,, \tag{8}$$

$$\Delta h(t) = \int_{t_0}^{t} G_h(t-t')\, RF^*(t')\, dt'\,, \tag{9}$$

where

$$G_T(t) = \alpha_T\, \mathrm{e}^{-t/\tau_T}\,, \tag{10}$$

$$G_h(t) = \alpha_h\, \mathrm{e}^{-t/\tau_h}\,, \tag{11}$$

with the parameters as given in Table II. The original parameter of Hasselmann et al. (1993) for sea level is $\alpha_h = (26.2/99.0)$ cm/yr. However, the coupled GCM that was used to derive the parameters includes only the sea level rise due to thermal expansion. In order to account for other effects, we increase the parameter to $\alpha_h = (50.0/99.0)$ cm/yr (Table II).

TABLE II

Coefficients of the impulse response functions G_T and G_h for the global mean surface temperature ΔT and sea level Δh changes, respectively

i	T	h
α_i	(2.246/36.8) K/yr	(50.0/99.0) cm/yr
τ_i	36.8 yr	99.0 yr

The climate response to aircraft-induced O_3 perturbations cannot be predicted from the corresponding radiative forcing as precisely as for well-mixed greenhouse gases like CO_2. The lifetime (adjustment time) of O_3 is only on the order of weeks. Hence, aircraft-induced O_3 changes are not well mixed (e.g., Dameris et al., 1998). Furthermore, the global mean surface temperature change cannot be predicted from the O_3 radiative forcing using the same climate sensitivity parameter as for CO_2 (Hansen et al., 1997; Ponater et al., 1999). The climate sensitivity parameter, which is the proportionality factor between radiative forcing and global mean equilibrium temperature response (IPCC, 1995), may be accurate only within a factor of two in the case of aircraft-induced O_3 perturbations.

In view of the rather long lifetime of CO_2, we account in an approximate manner for a radiative forcing of the O_3 changes caused by aircraft NO_x emissions. We call this forcing the (normalized) 'ozone' forcing $RF^*_{O_3}$, although it might also be used to include the radiative forcing from other radiatively active gases and particles that grow approximately linearly with aircraft emissions (due to relatively short lifetime).

In principle, the O_3 production rate non-linearly depends on the NO_x concentration with a maximum for the NO_x concentration between 100 and 1000 pptv (Ehhalt and Rohrer, 1995; Grooß et al., 1998). At some locations, where the background NO_x concentration is sufficiently high, this may result in a reduced O_3 production rate (or net O_3 destruction), as was demonstrated by Dameris et al. (1998). However, on the scale on which the aircraft NO_x emissions influence the O_3 production, these emissions are only a small perturbation for the NO_x budget. Hence, the mean O_3 concentration change depends quite linearly on the global aircraft NO_x emissions rate (Grewe et al., 1999). For simplicity, therefore, we assume that the radiative forcing of O_3 scales linearly with the NO_x emissions rate (similar to IPCC, 1990, p. 52):

$$RF^*_{O_3}(t) = \frac{S}{2.246} \times \frac{EI_{NO_x}(t)}{EI_{NO_x}(1992)} \times \frac{E_a(t)}{E_a(1992)} \,. \tag{12}$$

Here, $EI_{NO_x}(t)$ and $E_a(t)$ are the emissions index of nitrogen oxides per mass of fuel burnt and the aircraft fuel emissions rate, respectively. S is a scaling factor.

The factor 2.246 is used to normalize the radiative forcing to that of a doubling of CO_2. (Note: In our model, the equilibrium climate response to a CO_2 doubling is 2.246 K, cf. Table II.) We further assume that the temperature and sea level changes can be calculated analogously to (8) and (9), although RF^* is then replaced by $RF^*_{O_3}$.

The scaling factor S is the equilibrium temperature response (in K) due to O_3 induced by aircraft NO_x emissions in the year 1992. S is a *very* uncertain parameter. It comprises uncertainties both in the O_3 change due to aircraft NO_x emissions and in the climate response to an O_3 change. Using a comprehensive climate model, Ponater et al. (1999) calculated an equilibrium response of about 0.06 K for the O_3 perturbation caused by the 1991/92 air traffic. Due to a different O_3 change and a smaller climate sensitivity parameter, Rind (see Friedl, 1997) found a smaller value: 0.01 K for a reference O_3 change in 1992. He obtained 0.09 K for the O_3 change computed from a five times increased 1992 emissions rate. Ponater et al. (1998) found that the climate sensitivity parameter to aircraft-induced O_3 changes is about twice the climate sensitivity parameter for CO_2 forcing. Therefore, we chose $S = 0.05$ as a basis. Nevertheless, we also performed sensitivity studies with $S = 0.01$ and $S = 0.1$.

3. Emissions Scenarios

In the following, we consider various aircraft emissions scenarios, including CO_2 emissions and aircraft 'ozone' scenarios. (Table III). All these scenarios will be considered relative to a base (reference) case (denoted '*Scenario R*').

The temporal trend of the CO_2 concentration of the reference case is prescribed as observed since 1800 (IPCC, 1995, their Figure 1.5). An extrapolation according to scenario IS92a (IPCC, 1995) is used for the future until 2100. Data were kindly provided by Martin Heimann, based on work described in Enting et al. (1994).

In order to calculate the aircraft CO_2 emissions rate $E_a(t)$ in mass units of carbon per year, we use a carbon mass fraction of 0.86 in aviation fuels. The historical aircraft CO_2 emissions $E_a(t)$ (Table IV, Figure 1) are derived from data reported by the International Energy Agency (IEA, 1991) for aviation fuel production in the years 1960 to 1995. The IEA (1991) report lists the values only for specific years. The data have been completed for all years from 1971 to 1995 with the help of the OECD office in Bonn (pers. comm., 1997) and for the period 1960 to 1970 with input provided by A. Vedantham (pers. comm., 1997). Since the IEA data cover only a part of the world production for the years 1960 to 1970, data are increased by a factor 1.4. Any factor between 1.3 and 1.5 would give a reasonable continuity from 1970 to 1971. Fuel consumption is extrapolated backwards from 1960 assuming an annual growth rate of 8%. Any aviation fuel consumption before 1940 is neglected.

TABLE III

CO_2 emissions/concentration scenarios considered in this study

Name	Data basis for scenario	Duration
R	Reference (base) case: historical CO_2 concentration until 1995, IS92a thereafter (all natural and anthropogenic sources including aircraft emissions).	2100
Fa1	Standard aircraft emissions scenario: historic data (IEA) until 1995, NASA for 2015, FESGa (technology option 1) for 2050, 1% annual growth thereafter.	2100
Fa2	As *Fa1*, but for the technology option 2.	2100
Fe1	Aircraft emissions scenario: historic data (IEA) until 1995, NASA for 2015, FESGe (technology option 1) for 2050.	2050
Fc1	Aircraft emissions scenario: historic data (IEA) until 1995, NASA for 2015, FESGc (technology option 1) for 2050.	2050
Eab	Aircraft emissions scenario: historic data (IEA) until 1995, EDFa-base thereafter.	2100
Eah	Aircraft emissions scenario: historic data (IEA) until 1995, EDFa-high thereafter.	2100
C_τ	As *Fa1*, but aircraft emissions constant for $t \geq \tau$.	2100
N_{2015}	As *Fa1*, but no aircraft emissions after 2015.	2100

TABLE IV

Annual CO_2 emissions [Tg (C)] according to the aircraft emissions scenario *Fa1* for the years 1940 to 1995

Year / Decade	0	1	2	3	4	5	6	7	8	9
1940	7.7	8.3	9.0	9.7	10.5	11.3	12.3	13.2	14.3	15.4
1950	16.7	18.0	19.4	21.0	22.7	24.5	26.5	28.6	30.9	33.3
1960	36.0	39.5	43.5	45.9	48.0	51.3	55.6	65.6	74.3	77.8
1970	78.0	90.0	96.0	99.4	96.0	96.1	96.4	102.1	105.7	110.1
1980	110.9	109.3	110.5	112.0	119.5	123.4	129.9	135.6	141.4	146.5
1990	146.9	143.4	142.0	144.1	150.0	154.3				

TABLE V

Future annual CO_2 emissions [Tg (C)] according to the aircraft emissions scenarios *Fc1*, *Fa1*, *Fe1*, *Eab*, and *Eah*

Year	2015	2050	2100
Fc1	278.7	230.6	
Fa1	278.7	405.1	666.2
Fe1	278.7	640.1	
Eab	321.6	983.0	1276.2
Eah	524.6	1794.0	2045.1

According to these data, aviation emitted about 154 Tg(C)/yr in 1995, which corresponds to 2.4% of the 6300 Tg(C)/yr from fossil-fuel burn (Masood, 1997). The sum of all anthropogenic CO_2 emissions was about 8100 Tg(C)/yr in 1995 (6600 Tg(C)/yr due to industrial emissions, i.e., fuel burn and cement production, and 1500 Tg(C)/yr due to land-use changes; the values are listed for 1990 in Enting et al. (1994); they are extrapolated from 1990 to 1995 according to the IS92a scenario). Hence, aircraft contributed 1.9% to all anthropogenic emissions in 1995. The total aircraft CO_2 emissions from 1940 to 1995 amount to 4000 Tg(C). Based on an infinite geometric progression, this sum and the last emissions rate of about 154 Tg(C)/yr imply a mean annual increase rate of about 3.9%.

In the standard aircraft scenario (denoted '*Fa1*', see Table III), the future emissions in 2015 follow the NASA forecast (total emissions, Baughcum et al., 1998). However, the original values have been increased by 5% in order to account for a systematic underestimation (Baughcum, pers. comm.). The emissions in 2050 are those of the FESGa (technology 1) aircraft emissions scenario (FSEG, 1998; Baughcum et al., 1998; Schmitt and Brunner, 1997) provided for the forthcoming IPCC Special Report 'Aviation and the Global Atmosphere'. The FSEGa aircraft scenario corresponds to the economic growth assumed in the IS92a scenario for total emissions. It assumes a moderate growth rate of air traffic. Thereafter, until 2100, we assume that the fuel consumption increases further by a factor $1.01^{50} \approx 1.645$ compared to 2050, corresponding to an annual growth rate of 1%. Between the fixpoints 1995, 2015, 2050, and 2100 (cf. Table V), we use a linear interpolation for creating emissions scenario *Fa1*.

In addition to the standard aircraft scenario *Fa1*, we consider two other FESG-based scenarios: *Fc1* and *Fe1* (Figure 1, Table V). Here, the emissions for 2050 have been calculated assuming the economic growth corresponding to IS92c and IS92e, respectively. Nevertheless, we will compare these scenarios with the same reference scenario R (= IS92a) for the total emissions. These two scenarios are used to account for the uncertainties in the future development of aviation. The *Fc1*

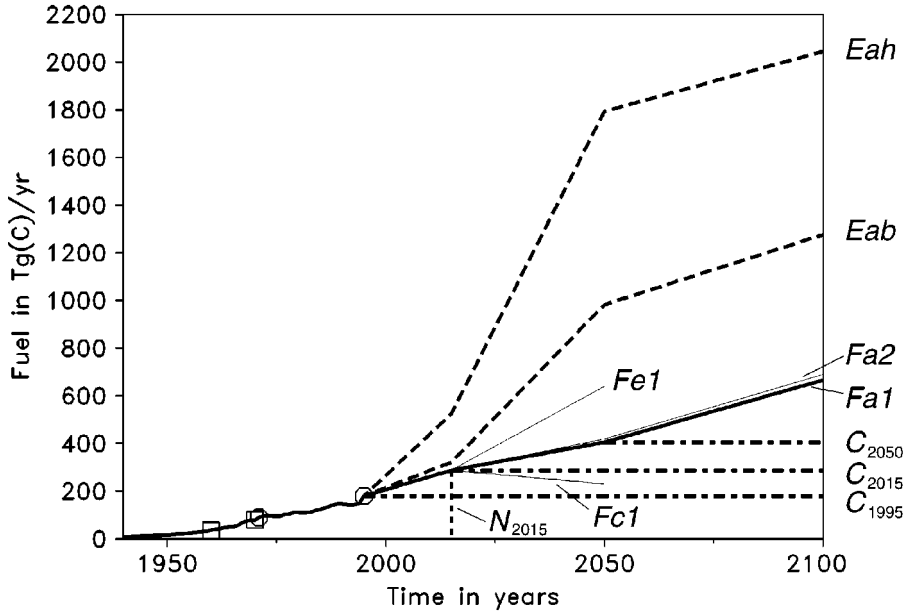

Figure 1. Aviation CO_2 emissions rate in mass units carbon per year versus time for various historical and future emissions scenarios listed in Table III. The full curve between the circles represents data on aviation fuel production as provided by IEA (1996) for the time period 1971 to 1995; the full curve between the square symbols denotes data of a similar kind, but with a less certain base.

and *Fe1* scenarios have not been extended to 2100. In addition, we consider two alternative scenarios, *Eab* and *Eah*, which are based on fixed year values (2015, 2050, 2100) of the EDF scenarios (Vedanthan and Oppenheimer, 1998) corresponding to IS92a (base-demand and high-demand cases). Again linear interpolation is used between the fixed year values.

In order to demonstrate the response of the climate system to a reduction in aircraft emissions, we have also constructed some drastic reduction scenarios (Figure 1):

- *Scenario* C_τ: The emissions follow scenario *Fa1* until year τ and are constant thereafter. We consider $\tau = 1995$, 2015, and 2050.
- *Scenario* N_{2015}: The emissions follow scenario *Fa1* until year 2015 and are zero thereafter.

We also study the impact of a NO_x reduction technology. While the *Fa1* scenario described above assumes a moderate progress in NO_x reduction based on conventional technology (technology option 1), the impact of an advanced low NO_x combustor technology (technology option 2), which gradually comes into service after 2015, is considered for the *Fa2* scenario. In this latter scenario, a 25% reduction in the NO_x emissions index is achieved for a 3.5% penalty in fuel (Table VI) based on the FESGa technology 2 scenario for 2050 (FESG, 1998). The *Fa1* and

TABLE VI

Future annual CO_2 [Tg(C)] and NO_x [Tg(NO_2)] emissions according to the aircraft emissions scenarios *Fa1* and *Fa2* (technology options 1 and 2)

Year	2015	2050	2100
CO_2 emissions, technology 1	278.7	405.1	666.2
technology 2	278.7	419.4	689.7
NO_x emissions, technology 1	4.67	7.16	11.77
technology 2	4.67	5.56	9.14

TABLE VII

Historical and future NO_x emissions indices [g(NO_2)/kg(fuel)] for the aircraft emissions scenarios *Fa1* and *Fa2* (technology options 1 and 2)

Year	1976	1984	1992	2015	2050	2100
Technology 1	9.8	11.0	12.0	13.4	15.2	15.2
Technology 2	9.8	11.0	12.0	13.4	11.4	11.4

Fa2 scenarios are identical until 2015, and split thereafter. The corresponding NO_x emissions indices are displayed in Table VII. The historical values and the 2015 number are taken from the NASA emissions inventory (Baughcum et al., 1998). The values for 2050 (technology options 1 and 2) are those from FESGa scenarios (FESG, 1998). We assume that the emissions index was constant before 1976 and will be constant after 2050. As for scenario *Fa1*, we extrapolate the fuel burn of scenario *Fa2* using a 1% annual growth rate after 2050. Between the fixpoints of Table VII, we interpolate linearly.

4. Results

4.1. CO_2 CONCENTRATION

Using (4) and (5), we calculated the aircraft contribution to CO_2 concentration for the various emissions scenarios listed in Table III. Aircraft emissions of the past (until 1995) caused a CO_2 increase of 1.4 ppmv, i.e., 1.7% of the total CO_2 concentration increase of 80 ppmv since 1800 (see also Figures 2 and 3, and Table VIII). A given CO_2 concentration threshold is obtained about 3.5 years later without aircraft emissions (according to scenario *Fa1*) than with aircraft emissions (Figure 3).

TABLE VIII

Atmospheric CO_2 concentration (from all anthropogenic emissions) and aircraft contributions to atmospheric CO_2 concentration according to various aircraft emissions scenarios (see Table III). Radiative forcing is also given for scenario *Fa1*

Year	CO_2 concentration [ppmv]										Rad. forc. [W/m^2]
	R	*Fc1*	*Fa1*	*Fe1*	*Eab*	*Eah*	C_{1995}	C_{2015}	C_{2050}	N_{2015}	*Fa1*
1800	280.8	0.00	0.00	0.00	0.00	0.00	0.00	0.00	0.00	0.00	0.000
1950	311.0	0.05	0.05	0.05	0.05	0.05	0.05	0.05	0.05	0.05	0.001
1970	324.6	0.35	0.35	0.35	0.35	0.35	0.35	0.35	0.35	0.35	0.007
1990	353.3	1.13	1.13	1.13	1.13	1.13	1.13	1.13	1.13	1.13	0.021
1992	356.7	1.22	1.22	1.22	1.22	1.22	1.22	1.22	1.22	1.22	0.022
1995	361.8	1.37	1.37	1.37	1.37	1.37	1.37	1.37	1.37	1.37	0.024
2000	370.4	1.69	1.69	1.69	1.70	1.76	1.66	1.69	1.69	1.69	0.029
2015	400.8	2.87	2.87	2.87	3.01	3.81	2.45	2.87	2.87	2.87	0.046
2050	497.1	5.19	6.32	7.84	10.33	17.25	3.97	5.56	6.32	2.14	0.068
2100	685.3		13.16		25.27	42.41	5.71	8.52	10.88	1.65	0.082

In the case of standard aircraft emissions (scenario *Fa1*), aircraft contribution to CO_2 concentration grows more rapidly than the total CO_2 concentration does, and reaches 6.3 and 13.2 ppmv in the years 2050 and 2100, respectively (Figure 2). Hence, the relative contribution of aircraft to the anthropogenic CO_2 concentration increases from 1.7% in 1995 to 2.9% in 2050 and to 3.2% in 2100 (Figure 4), i.e., the aircraft-induced fraction of the atmospheric CO_2 concentration nearly doubles during the next century. The corresponding radiative forcing according to (7) is also given in Table VIII.

The various (non-academic and potentially realistic) aircraft emissions scenarios result in a large range of values for the concentration increase (Figure 2), ranging from 5.2 to 17.3 ppmv in 2050 and from 13.2 to 42.4 ppmv in 2100, i.e., from 3.2% to more than 10% of the change in the reference IPCC scenario *R* (Figure 4). In particular, the *Eab* and *Eah* scenarios exhibit a rather rapid growth of the relative aircraft contribution until 2050, with a slower growth thereafter due to saturation effects in traffic demand (10.5% for *Eah* in 2100). Compared to the EDF scenarios, the spread of the FESG scenarios is small.

In the constant emissions scenario C_τ, the aircraft-induced atmospheric CO_2 concentrations grow further after the emissions are frozen, although less rapidly than for scenario *Fa1* (Figure 5). In 2100, the concentrations are larger by factors 4.2, 3.0, and 1.7 than the aircraft-induced concentration at times at which emissions are kept constant for the scenarios C_{1995}, C_{2015} and C_{2050}, respectively. The corres-

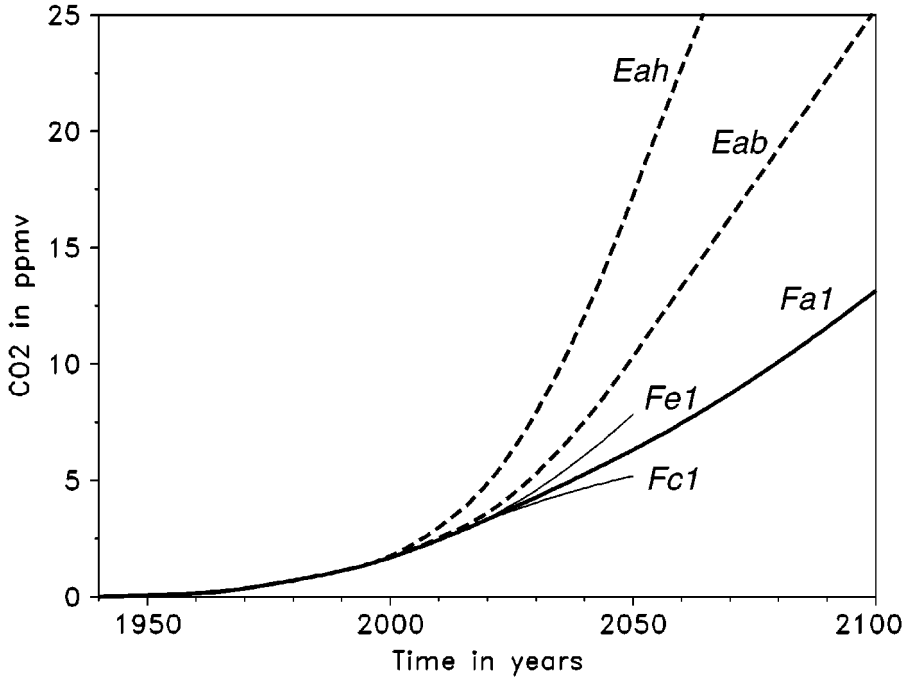

Figure 2. Aircraft contribution to the atmospheric CO_2 concentration versus time for the realistic emissions scenarios of Table III.

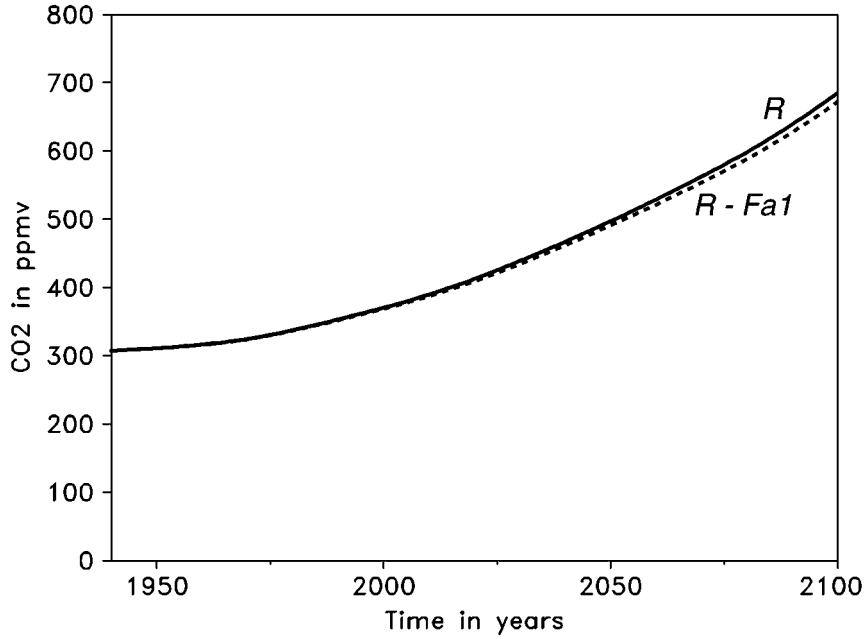

Figure 3. Atmospheric CO_2 concentration versus time due to all anthropogenic emissions (scenario *R*, full curve) and due to all anthropogenic emissions except aircraft (*R* minus *Fa1*, dashed).

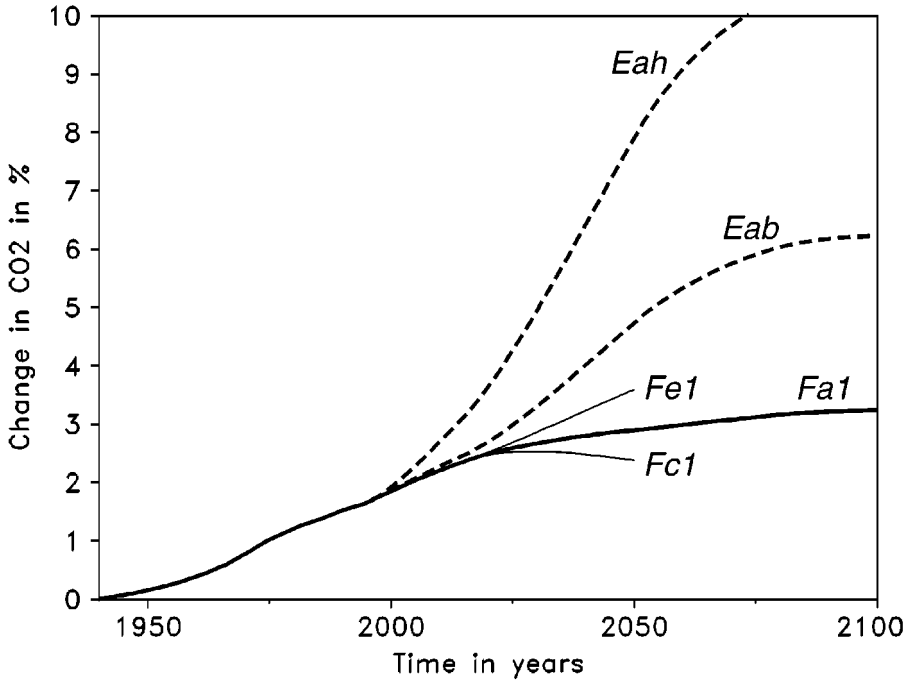

Figure 4. Change in CO_2 concentration due to aircraft emissions (according to the realistic scenarios of Table III) relative to the total increase since 1800.

ponding relative contributions to the overall CO_2 increase since 1800 are plotted in Figure 6.

Only in the case of scenario N_{2015}, does the aircraft-induced atmospheric CO_2 concentration decrease immediately after 2015 (Figures 5 and 6). From 2015 to 2100, the aircraft contribution to the CO_2 concentration drops from 2.9 ppmv to 1.6 ppmv, which is still higher than the aircraft-induced CO_2 concentration in 1995 (1.4 ppmv).

4.2. TEMPERATURE AND SEA LEVEL

Using the formulae (6) and (8) to (11), the changes in global mean surface temperature and global mean sea level due to CO_2 concentration changes are calculated for the various CO_2 concentration scenarios listed in Table III.

Figures 7 and 8 show the temperature and sea level changes, respectively, since 1800 for the base case, i.e., scenario *R* (see also Tables IX and X). Due to the approximately exponentially increasing CO_2 concentration and its logarithmic impact on radiative forcing, the surface warms linearly with time after a spin-up period. The temperature change is 2.2 K in 2100. The corresponding sea level rise is 31 cm.

According to IPCC (1996), the best estimate values for changes in 2100 in the IS92a scenario are about a 2 K temperature change and a 50 cm sea level change, if

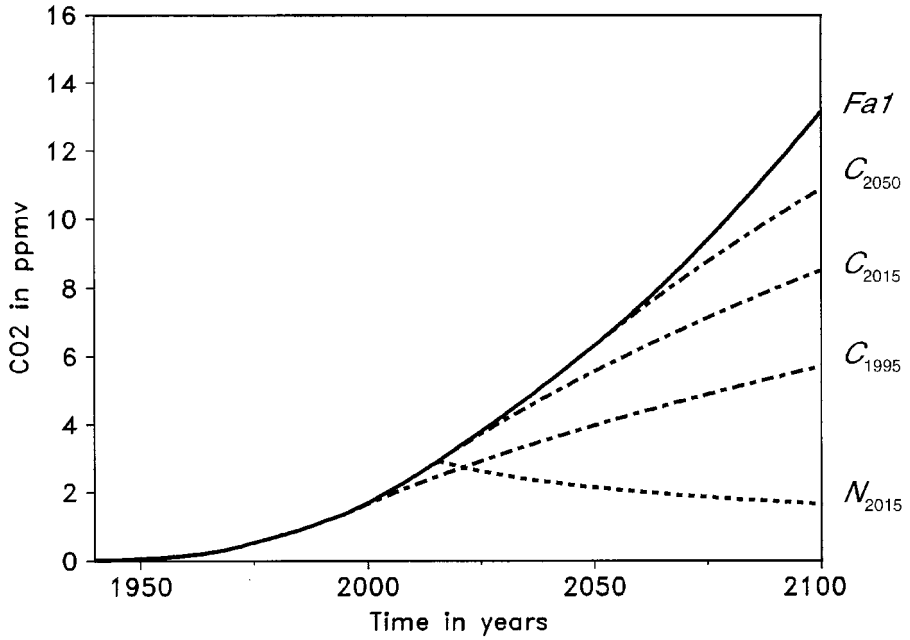

Figure 5. Aircraft contribution to the atmospheric CO_2 concentration versus time for the artificial emissions scenarios of Table III.

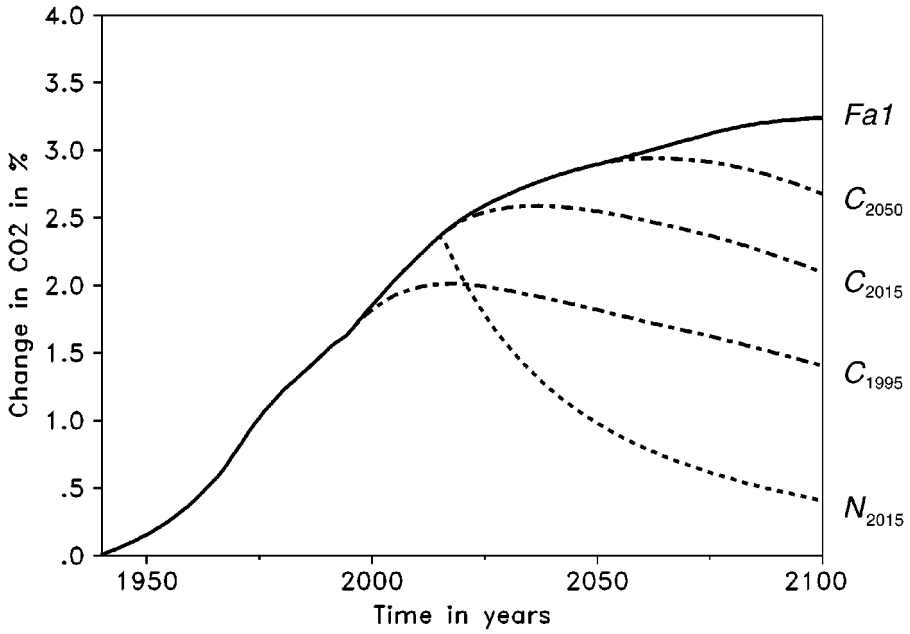

Figure 6. Change in CO_2 concentration due to aircraft emissions (according to the scenarios of Table III) relative to the total increase since 1800.

TABLE IX

Temperature change since 1800 for various CO_2 emissions scenarios (see Table III)

Year	Temperature change [K]									
	R	*Fc1*	*Fa1*	*Fe1*	*Eab*	*Eah*	C_{1995}	C_{2015}	C_{2050}	N_{2015}
1950	0.232	0.000	0.000	0.000	0.000	0.000	0.000	0.000	0.000	0.000
1970	0.305	0.001	0.001	0.001	0.001	0.001	0.001	0.001	0.001	0.001
1990	0.437	0.003	0.003	0.003	0.003	0.003	0.003	0.003	0.003	0.003
1992	0.455	0.004	0.004	0.004	0.004	0.004	0.004	0.004	0.004	0.004
1995	0.483	0.004	0.004	0.004	0.004	0.004	0.004	0.004	0.004	0.004
2000	0.532	0.006	0.006	0.006	0.006	0.006	0.006	0.006	0.006	0.006
2015	0.702	0.010	0.010	0.010	0.010	0.011	0.010	0.010	0.010	0.010
2050	1.230	0.023	0.025	0.028	0.033	0.050	0.018	0.024	0.025	0.015
2100	2.159		0.047		0.086	0.146	0.025	0.036	0.043	0.011

TABLE X

Sea level rise since 1800 for various CO_2 emissions scenarios (see Table III)

Year	Sea leavel change [cm]									
	R	*Fc1*	*Fa1*	*Fe1*	*Eab*	*Eah*	C_{1995}	C_{2015}	C_{2050}	N_{2015}
1950	3.146	0.001	0.001	0.001	0.001	0.001	0.001	0.001	0.001	0.001
1970	4.207	0.007	0.007	0.007	0.007	0.007	0.007	0.007	0.007	0.007
1990	5.933	0.034	0.034	0.034	0.034	0.034	0.034	0.034	0.034	0.034
1992	6.157	0.038	0.038	0.038	0.038	0.038	0.038	0.038	0.038	0.038
1995	6.510	0.045	0.045	0.045	0.045	0.045	0.045	0.045	0.045	0.045
2000	7.142	0.058	0.058	0.058	0.058	0.058	0.058	0.058	0.058	0.058
2015	9.374	0.109	0.109	0.109	0.111	0.121	0.104	0.109	0.109	0.109
2050	16.713	0.278	0.298	0.324	0.376	0.549	0.230	0.285	0.298	0.195
2100	31.361		0.653		1.120	1.864	0.378	0.522	0.611	0.209

only greenhouse gases are considered. Note that the present model study includes the impact of CO_2 emissions only and does not include the radiative forcing due to other trace gases such as methane and ozone. The IPCC value for the sea level rise is approximately met with our choice of parameters in the response function for the sea level (Table II).

The temperature and sea level changes are plotted in Figures 9 and 10, respectively, for the standard aircraft emissions scenario *Fa1*. Aircraft contributions to global warming are 0.004, 0.010, 0.025, and 0.047 K for 1995, 2015, 2050, and 2100, respectively (Table IX). The corresponding sea level changes are 0.045, 0.11,

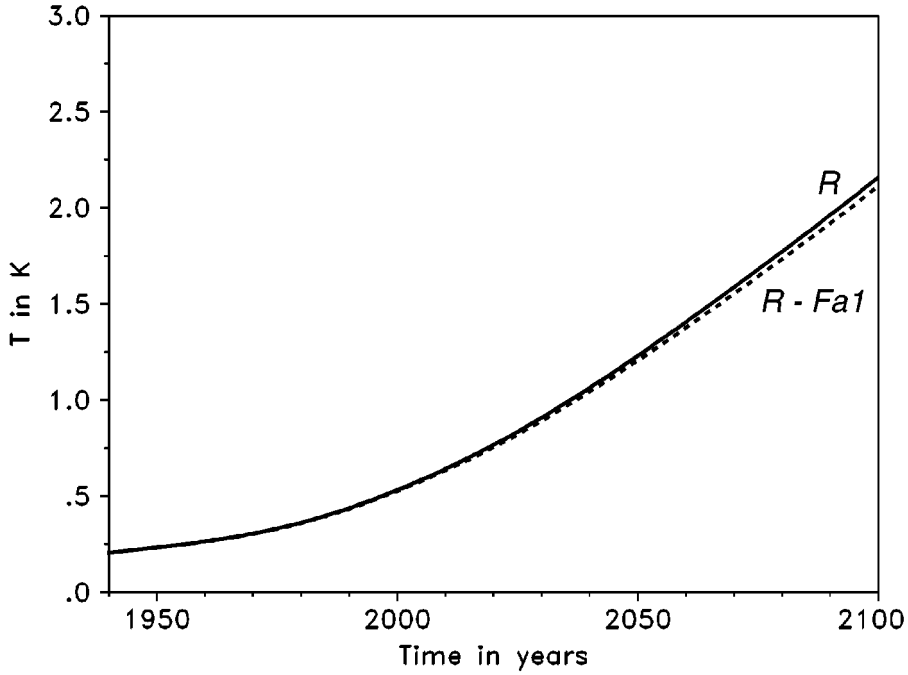

Figure 7. Global surface temperature change (since 1800) versus time due to total CO_2 emissions (scenario *R*, full curve) and total change minus aircraft-induced change (*R* minus *Fa1*, dashed).

0.30, and 0.65 cm (Table X). The aircraft contribution to the overall temperature and sea level changes remains small, as can be inferred from Figures 7 and 8. We note that aircraft emissions shift the increases by a few years (2.5 years for temperature and 2.2 years for sea level) to earlier times. The shift is shorter than for the CO_2 concentration (cf. Section 4.1). The relative importance of the aircraft emissions for the anthropogenic changes grows with time (Figure 11) from 0.9 (0.7) % in 1995 to 2.2 (2.1) % in 2100 in the case of global mean surface temperature (global mean sea level rise).

The responses depend strongly on the assumed scenarios, which is to be expected. Apparently, the scenarios *Fc1* and *Fe1* span only a small range of the potential response. Larger responses are implied by the scenarios *Eab* and *Eah*. While the temperature response due to CO_2 emissions from aircraft remains relatively small in scenario *Fa1* (2.2% of the anthropogenic warming according to scenario *R*), it will be different for scenario *Eah* by the end of the next century (6.8% of the anthropogenic temperature rise).

In the case of scenarios with constant aircraft emissions (C_τ), the aircraft-induced temperature change (Figure 12) and sea level rise (Figure 13) are less pronounced than in scenario *Fa1*. Nevertheless, the temperature and sea level still grow considerably after the emissions rates are kept constant. In the year 2100, the

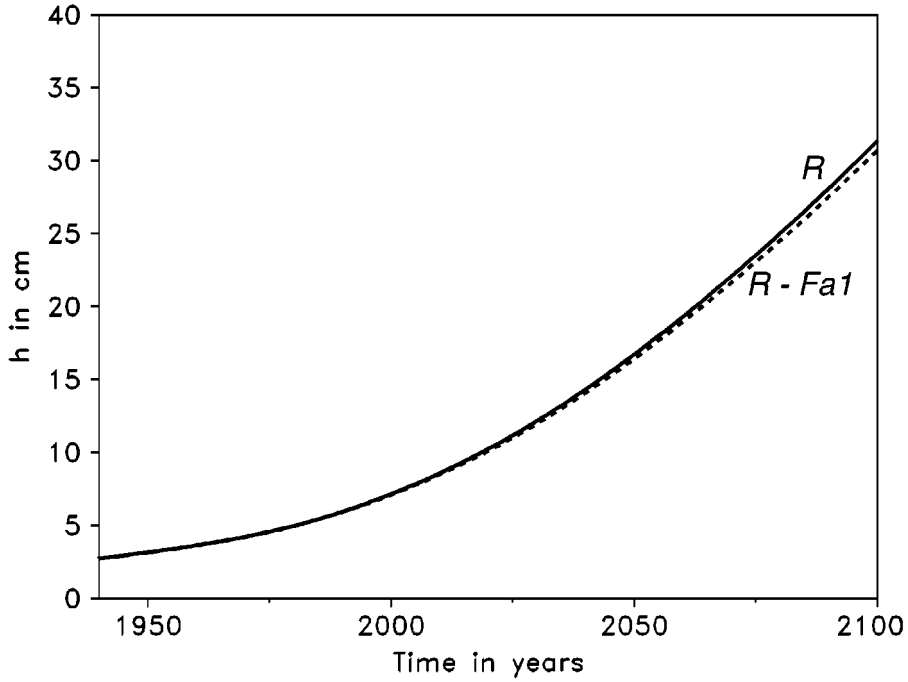

Figure 8. Global sea level change (since 1800) versus time due to total CO_2 emissions (scenario *R*, full curve) and total change minus aircraft-induced change (*R* minus *Fa1*, dashed).

temperature changes are 0.025, 0.036, and 0.043 K for the scenarios C_{1995}, C_{2015}, and C_{2050}, respectively. The corresponding sea level rises are 0.4, 0.5, and 0.6 cm.

In the case of no aircraft CO_2 emissions after 2015 (scenario N_{2015}), both the warming and the sea level rise continue far beyond 2015 (Figures 12 and 13). In the case of temperature, the aircraft-induced warming of year 2015 is again not obtained before 2100. In the case of sea level, this point is reached even later.

4.3. OZONE-INDUCED CLIMATE CHANGE

The aircraft-induced temperature change due to ozone perturbations can be predicted from NO_x emissions by equations (8)–(11) with (12). The results for selected combinations of aircraft emissions scenarios (see Table III) and scaling factors S are given in Table XI. (Remember that S is equivalent to the equilibrium temperature response in K to the 1992 O_3 forcing.) Also, the CO_2-induced temperature change (for scenario *Fa1*) is listed in Table XI.

In the case of standard emissions scenario *Fa1*, Figure 14 compares aircraft-induced temperature changes due to CO_2 emissions with the temperature change due to O_3 perturbation, i.e., due to NO_x emissions. If the scaling factor is $S = 0.05$, O_3-induced temperature changes are 0.023, 0.048, 0.111, and 0.215 K for

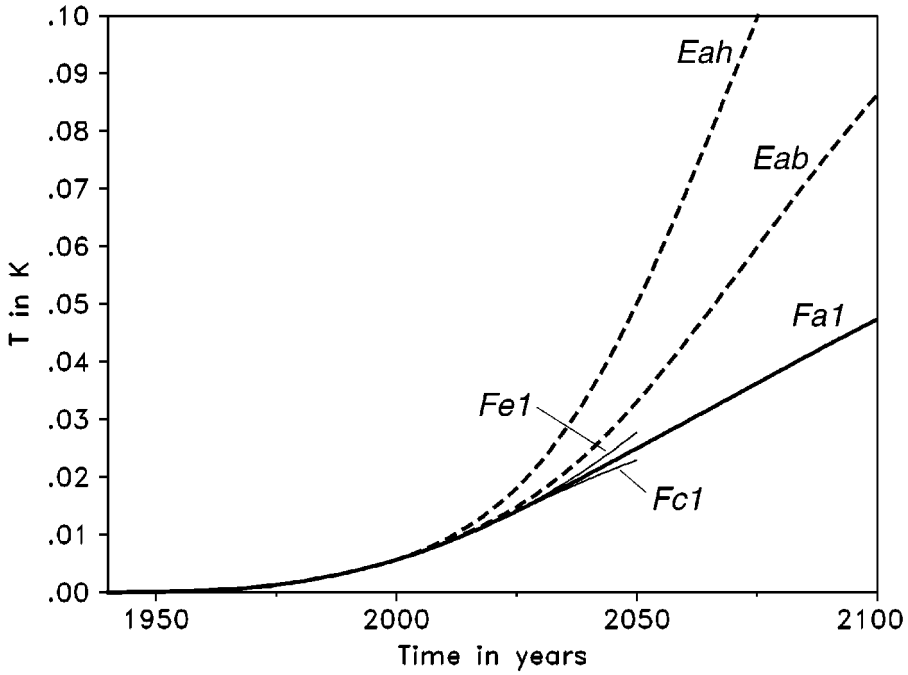

Figure 9. Aircraft CO_2 contribution to the global mean surface temperature change in K versus time for the realistic emissions scenarios of Table III.

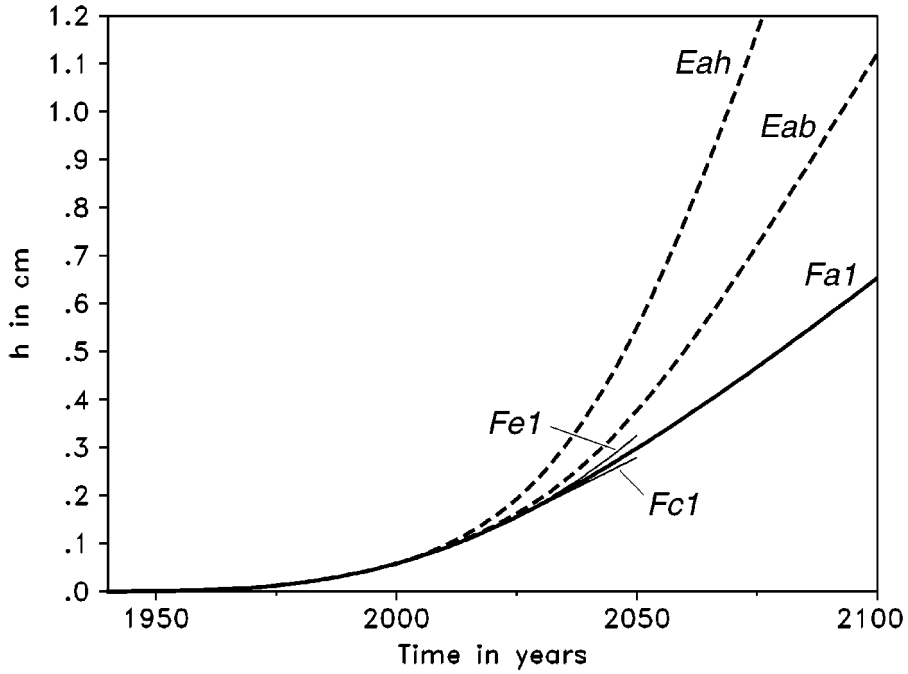

Figure 10. Aircraft CO_2 contribution to the global mean sea level rise in cm versus time for the realistic emissions scenarios of Table III.

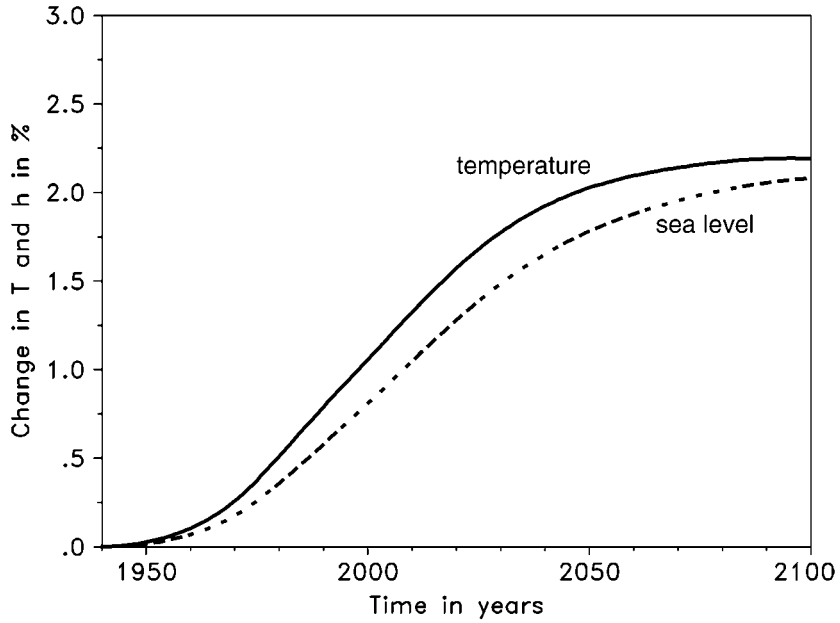

Figure 11. Relative aircraft contributions (according to scenario *Fa1*) to the changes in the global mean surface temperature (full curve) and the global mean sea level rise (dashed curve).

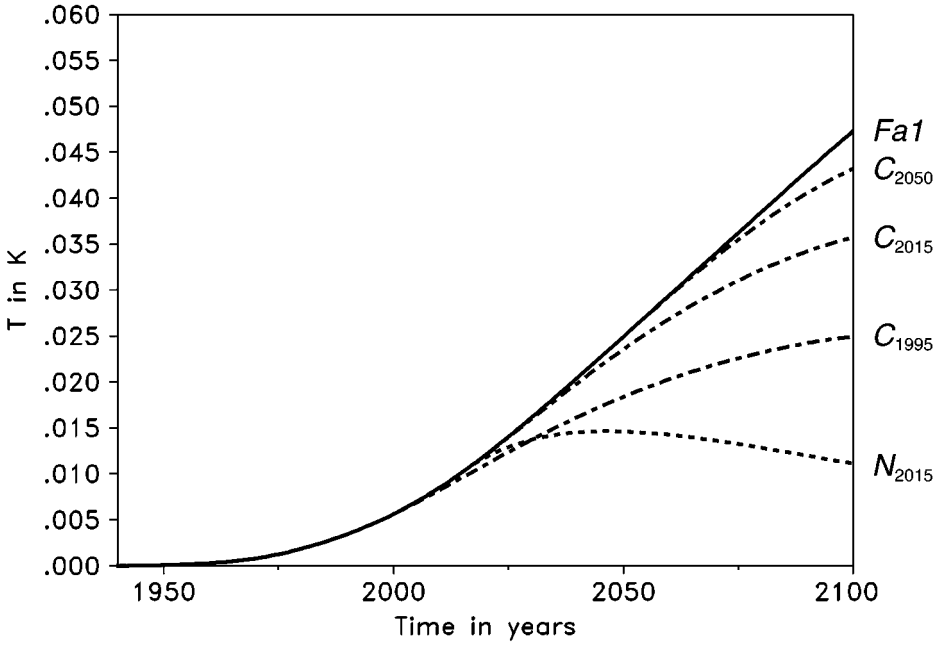

Figure 12. Aircraft CO_2 contribution to the global mean surface temperature change in K versus time for the artificial emissions scenarios of Table III.

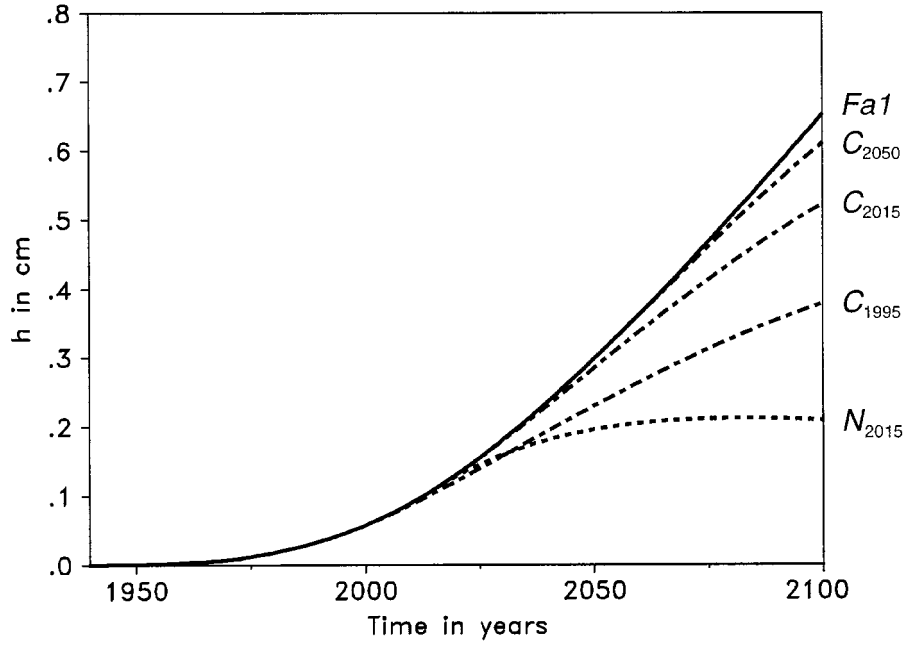

Figure 13. Aircraft CO_2 contribution to the global mean sea level rise in cm versus time for the artificial emissions scenarios of Table III.

TABLE XI

Temperature changes [K] (separately due to CO_2 and NO_x-induced O_3) since 1800 for several aircraft emissions scenarios (see Table III) and scaling factors S

Year	*Fa1* CO_2	*Fa1* O_3			C_{2015} O_3	N_{2015} O_3
		$S = 0.01$	$S = 0.05$	$S = 0.10$	$S = 0.05$	$S = 0.05$
1995	0.004	0.005	0.023	0.045	0.023	0.023
2015	0.010	0.010	0.048	0.097	0.048	0.048
2050	0.024	0.022	0.111	0.221	0.091	0.019
2100	0.047	0.043	0.215	0.431	0.116	0.005

1995, 2015, 2050, and 2100, respectively. The O_3-induced temperature change is significantly larger than the CO_2-induced temperature change, for $S \geq 0.02$.

In the case of scenario C_{2015} (Figure 15), the temperature change due to O_3 perturbation approaches slightly more rapidly its equilibrium than the CO_2-induced temperature change does. In the case of scenario N_{2015}, the temperature change due to the O_3 perturbation decreases immediately after 2015, whereas the CO_2-induced temperature change still increases.

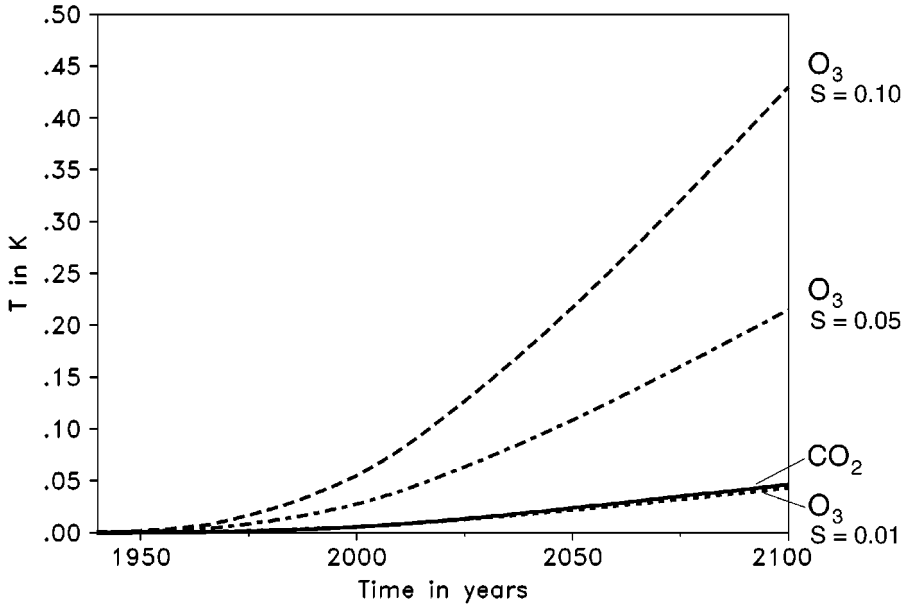

Figure 14. Aircraft-induced temperature changes in K due to CO_2 emissions (full curve) and due to O_3 perturbation (without CO_2 part, dashed curves) for the standard emissions scenario *Fa1*, and for several scaling factors $S = 0.01$, 0.05, and 0.1.

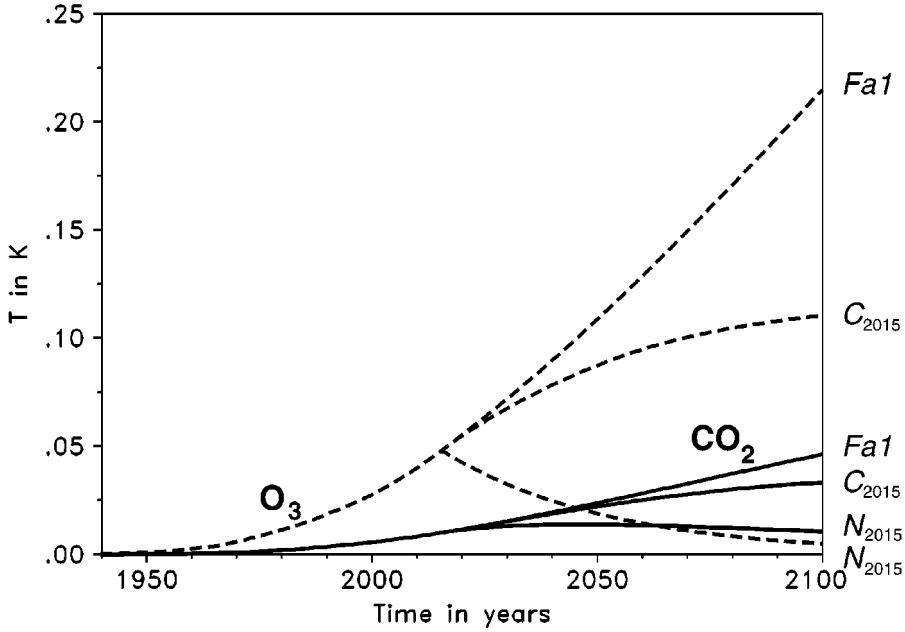

Figure 15. Aircraft-induced temperature changes in K separately due to CO_2 emissions (full curves) and due to O_3 perturbations (dashed curves) for the scenarios *Fa1*, C_{2015}, and N_{2015}. The scaling factor is $S = 0.05$.

Far larger temperature changes are expected for the scenarios *Eab* and *Eah* compared to *Fa1*.

4.4. TRANSIENT VERSUS EQUILIBRIUM SIMULATIONS

Atmospheric general circulation models with prescribed sea surface temperature (e.g., Sausen et al., 1997) or with the sea surface temperature determined from a model of the oceanic mixed layer (e.g., Rind et al., 1996; Ponater et al., 1999) have been used in order to calculate the climate change due to aircraft-induced O_3 changes. These models are usually run in the equilibrium mode, i.e., the equilibrium response is calculated to a forcing (or greenhouse gas perturbation) constant in time.

In the real world as in the scenarios of the present paper, the concentration of greenhouse gases changes gradually. Therefore, transient climate simulations are required and equilibrium simulations can only provide a first estimate of the effect. In any scenario with increasing emissions or with increasing and then constant emissions, the instantaneous climate change signal at a given time t_a will be smaller than the equilibrium climate response obtained for the radiative forcing at time t_a. Here, the question arises whether the climate signal due to aircraft-induced CO_2 and O_3 perturbations are overestimated by the same factor. Our linear response model is a suitable tool to provide an answer to such a question.

All simulations previously reported in this paper were performed in the transient mode with time-dependent forcings. In the case of temperature, the equilibrium response ΔT_{equi} to a constant forcing $RF^*(t_a)$ is obtained from Equation (8) by moving t to ∞:

$$\Delta T_{\text{equi}} = \alpha_T \, \tau_T \, RF^*(t_a) \, . \tag{13}$$

An analogous result can be calculated for the sea level rise.

Table XII compares the transient and the equilibrium temperature responses, computed from Equations (8) and (13), due to aircraft-induced CO_2 and O_3 perturbations for selected years. In the coming century, the transient response is typically 35% to 75% of the equilibrium response, and the ratio increases with time. The ratios for the CO_2 and O_3 perturbations are of similar magnitude. These results are dependent on the functional form (not the magnitude) of the forcing, i.e., the CO_2 concentration and the NO_x emissions rate.

4.5. COMPARISON OF TWO TECHNOLOGY SCENARIOS

Engineers have the option to optimize aircraft combustors with respect to either minimum fuel consumption or minimum nitrogen oxides (NO_x) emissions. The two technology options (1 and 2), i.e., scenarios *Fa1* and *Fa2* (see Tables VI and VII), have been set-up by FESG (1998) to allow for tests of the consequences of a low NO_x combustor technology (as assumed for scenario *Fa2*). Using our

TABLE XII

Transient and equilibrium temperature changes [K] since 1800 due to CO_2 and O_3 perturbations according to the standard aircraft emissions scenario *Fa1*. The ratio of the transient and equilibrium temperature changes is also listed. The scaling factor is $S = 0.05$

Year	Trans. temp. change		Equil. temp. change		Trans./equil. ratio	
	CO_2	O_3	CO_2	O_3	CO_2	O_3
1995	0.004	0.023	0.012	0.055	0.36	0.41
2015	0.010	0.048	0.022	0.110	0.44	0.44
2050	0.024	0.111	0.041	0.181	0.60	0.61
2100	0.047	0.215	0.062	0.297	0.75	0.73

TABLE XIII

Fuel consumption, nitrogen oxides emissions indices EI_{NO_x}, and temperature changes T, separately due to CO_2 and O_3, for the two technology options represented by *Fa1* (conventional combustors) and *Fa2* (low NO_x combustors). The scaling factor for the temperature response via O_3 is $S = 0.05$

Year	Fuel burn [Tg(C)/year]		EI_{NO_x} [g/kg]		ΔT due to CO_2 [K]		ΔT due to O_3 [K]	
	Fa1	*Fa2*	*Fa1*	*Fa2*	*Fa1*	*Fa2*	*Fa1*	*Fa2*
1940	12	12	9.8	9.8	0.000	0.000	0.000	0.000
1976	96	96	9.8	9.8	0.002	0.002	0.011	0.011
1984	120	120	11.0	11.0	0.003	0.003	0.015	0.015
1992	142	142	12.0	12.0	0.005	0.005	0.022	0.022
2015	279	279	13.4	13.4	0.011	0.011	0.049	0.049
2050	405	419	15.2	11.4	0.025	0.025	0.111	0.098
2100	666	690	15.2	11.4	0.047	0.048	0.216	0.170

linear response model, temperature changes are computed separately for CO_2 and O_3 forcings, and are listed in Table XIII. The scaling factor, see (12), for the O_3 response has been chosen as $S = 0.05$. The sum of the CO_2- and O_3-induced temperature changes is plotted in Figure 16.

The radiative forcings and the temperature changes due to CO_2 are rather similar for both technologies (slightly smaller for technology 1 option, *Fa1*). If $S = 0.05$, the temperature change due to O_3 increases more rapidly than that due to CO_2. However, it is only after 2050 that the low NO_x technology (technology 2, *Fa2*) results in a stronger reduction in temperature change. While the reduction in 2050 is 12%, it amounts to 21% in 2100.

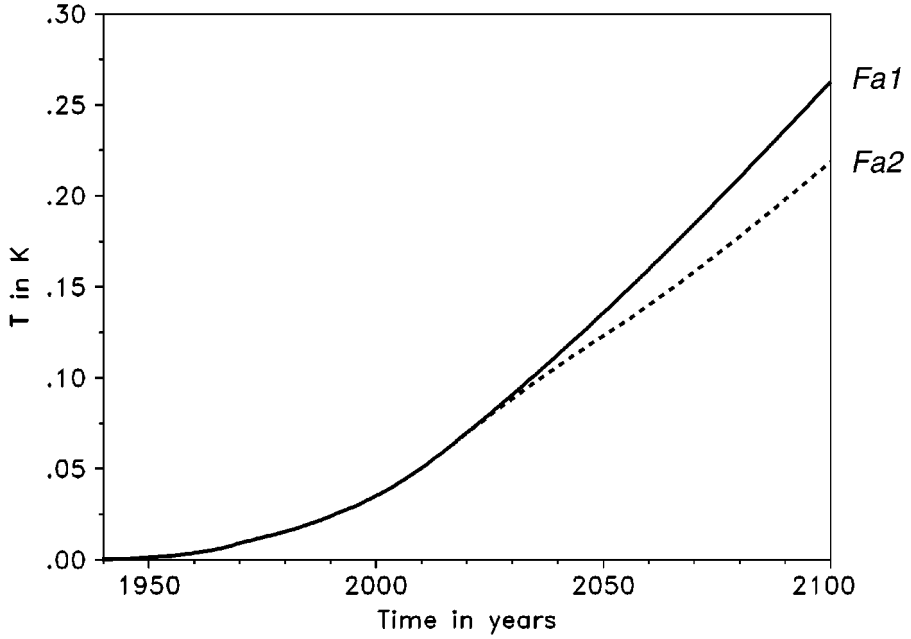

Figure 16. Temperature changes from 1940 to 2100 induced by CO_2 and O_3 for different technology options as represented by scenarios *Fa1* (full curve) and *Fa2* (dashed curve). The scaling factor is $S = 0.05$.

The low NO_x technology (*Fa2*) results in a smaller climate change, despite the fact that this technology requires a larger fuel burn and, hence, emits more CO_2: a total temperature change of 0.22 K is calculated for the year 2100 (*Fa2*), whereas the conventional technology (*Fa1*) results in 0.26 K. Even for a small scaling factor, $S = 0.01$, low NO_x technology is beneficial for a sustainable climate: global mean temperature rises by 0.082 and 0.090 K in the year 2100 for the technology 2 and 1 options, respectively.

It should be noted that the magnitude of the difference between the technology options strongly depends on the scaling factor S, which has been introduced to account for uncertainties with respect to the climate impact of aircraft NO_x emissions. These uncertainties are much larger than for the impact of aircraft CO_2 emissions. Furthermore, the quantitative results are also dependent on the functional form of the emissions scenarios.

5. Uncertainties

The results depend on many details of the model and its input. Here, we discuss a few of them in relation to other data and results available in the literature.

TABLE XIV

Response function values $G_C(t)$ (normalized to unity at time zero) for various times t and models. This study uses model RW1

t [yr]	Model			
	RW0	RW1	IPERT	IP90
0	1.00	1.00	1.00	1.00
10	0.84	0.78	0.64	0.62
100	0.54	0.41	0.41	0.31
200	0.38	0.30	0.39	0.25

5.1. CARBON CYCLE MODEL

Many studies have been performed to determine the CO_2 concentration change due to anthropogenic carbon dioxide emissions. Reviews are given by, e.g., Siegenthaler and Joos (1992), Enting et al. (1994), and Joos et al. (1996). The physics of the carbon cycle is non-linear, so that any linear model is applicable only for a certain range of concentrations and emissions scenarios (Joos et al., 1996). Various linearized models have been proposed for scenario studies. Examples include the atmospheric response models RW0 and RW1 of Hasselmann et al. (1997), based on Maier-Reimer (1987) and on Maier-Reimer and Hasselmann (1987), or the models IPERT and IP90 recommended by Enting et al. (1994) as reference models for global warming potential calculations in the IPCC (1996) study. Table XIV lists the values of the normalized response functions $G_C(t)$ for various times t. We see that the response function values differ by more than 20% on relevant times scales. The model RW1 selected for this study falls within the range of other models.

Table XV lists the CO_2 concentration responses for aviation scenario *Fa1* at various times for the four considered models. The results of model RW1 differ by about 10 to 20% from the results for other response models. This characterizes the range of uncertainty due to the carbon cycle for the choice of the model. Model RW1 implies a mean sensitivity of 0.00024 ppmv/Tg(C) on average over the time period up to 2100 for reference scenario *Fa1*, which is in the range of the models used for IPCC (1996).

5.2. PAST AND FUTURE FUEL CONSUMPTION DATA

The climatic response to CO_2 emissions from aircraft at a given time depends on the history and the future of emissions over time scales of the carbon cycle and of the temporal evolution of aviation. Hence, it is important to assess the validity of the data on past and future fuel consumption by aviation.

TABLE XV

Carbon dioxide concentration increase [ppmv] due to aviation emissions at various times for various models, for scenario $Fa1$

t [yr]	Model			
	RW0	RW1	IPERT	IP90
1995	1.49	1.37	1.14	1.11
2015	3.18	2.87	2.38	2.29
2050	7.22	6.32	5.24	4.89
2100	15.43	13.16	11.24	10.08

Historical fuel burn data are listed in Table XVI. The IEA data used here are compared to other published data. The various studies are either based on detailed analysis of air traffic and aircraft-specific fuel consumption (e.g., Baughcum et al., 1996a,b, 1998; Gardner et al., 1997, 1998; Schmitt and Brunner, 1997) or derived from data on fuel consumption by aviation in one or a few specific years and estimated temporal trends (e.g., Nüsser and Schmitt, 1990; Brasseur et al., 1998). The IEA values define the production of fuels suitable for aviation, but may overestimate the consumption of these fuels by aviation (Baughcum et al., 1996a; Gardner et al., 1997). On the other hand, the detailed analyses underestimate the fuel consumption as they assume idealized flight altitudes and routes (great circles, no wind, no holdings, no conflicts with other air traffic, etc.). As noted before, the IEA data are based on data collected from various regions of the world, and the global cover increased in 1970. This was accounted for by a correction factor 1.4 for the global production data before 1970. Moreover, we had to guess at the temporal evolution of fuel consumption in the time period before 1960. However, the integrated fuel consumption before 1960 (1970) amounts to less than 11 (33)% of the total fuel consumption until 1995. Therefore, the IEA data seem to provide a reasonable upper bound for past fuel consumption by aviation. The estimated uncertainty in the amount of past fuel consumption since the beginning of aviation is on the order of 20%.

The present study uses a wide set of scenarios which are likely to embrace the lowest and highest growth rates to be expected for the future. First, the future responses will increase in proportion to the emission rates. Reference scenario *Fa1* used in this study is not an extreme one. Scenarios *Eab* and *Eah* imply 1.9 and 3.1 times larger emissions in the year 2100. The study of Vedantham and Oppenheimer (1998) describes one even larger scenario with fuel consumption that is 4.5 times larger than the value used for *Fa1* in 2100. Since we cannot assess the plausibility of these various scenarios, there is clearly a large source of uncertainty in assessing future trends.

TABLE XVI
Aircraft fuel consumption rates [Tg(fuel)/yr] from different sources

Year of fuel consumption	1976	1984	1988	1992	2015
IEA (1996)	111.8	138.2	161.3	170.8	
Nüsser and Schmitt (1990)			150		
Baughcum (pers. comm.)	100.0	116.3		139.4	308.6
Gardner et al. (1997)				165	
Schmitt and Brunner (1997)				129.3	285
Brasseur et al. (1998)	98.2	120.0	130.9	141.8	
Gardner et al. (1998)				131.3	286.9

5.3. COMPARISONS OF COMPUTED RESPONSES

Friedl (1997) and Brasseur et al. (1998) reviewed studies that have been performed in order to determine the induced ozone increase in the atmosphere and the resultant radiative forcing due to NO_x emissions from aviation. The studies agree in the conclusion that subsonic aircraft NO_x emissions increase the O_3 concentration in the upper troposphere, but they differ largely in the assumed emissions, the amount of O_3 increase, the radiative forcing, and the resultant temperature change at the Earth's surface. The reported radiative forcing values vary between 0.01 Wm^{-2} (Friedl, 1997) and 0.05 Wm^{-2} (Hauglustaine et al., 1994). However, only two studies are known where a global circulation model has been applied to determine the equilibrium global mean surface temperature change. These studies report temperature changes of 0.01 K for 1992 aviation's emissions, 0.09 K for a five-fold increase in these emissions (Rind in Friedl, 1997), and 0.06 K for 1992 emissions (Ponater et al., 1999). These models do not account for recently discussed feedback mechanisms by which increased nitrogen oxides emissions reduce the lifetime of methane and hence lead to a reduction in the overall greenhouse effect.

Table XVII lists the fuel consumption for specific years, the estimated CO_2 concentration changes due to aviation, the corresponding radiative forcings, the temperature changes, and the average past fuel consumption increase rates. The integrated fuel consumption of the past as reported by Friedl (1997) is about a factor 2 smaller than the values in the present study. When scaled with the total fuel consumption, the various estimates are not significantly different.

Hence, the state of the art does not yet allow for a detailed assessment of the uncertainty in computed radiative forcing. As a consequence, the uncertainty of the present results on the global mean temperature change at the Earth's surface due to aircraft-induced O_3 changes is even less known. We can only say that the scaling factors S of 0.01 to 0.1 (i.e., the equilibrium temperature change due to

TABLE XVII

Comparison of the changes in CO_2-related variables due to aviation: fuel burn, CO_2 concentration change, radiative forcing, temperature change, and annual increase rate of fuel burn

Reference	Year	Fuel [Tg/yr]	Total C [Tg (fuel)]	ΔC_{Fa1} [ppmv]	RF_{Fa1} [Wm^{-2}]	ΔT_{Fa1} [K]	Fuel increase
Friedl (1997)	1990	134	2000	0.5	0.0067	0.007 (0.0025 – 0.009)	4.6%/yr
Brasseur et al. (1998)	1995	150	3550	1.35	0.027	0.008	linear from 1940 to 1995
Present study	1990	170.8	3800	1.13	0.021	0.0034	IEA (4.5%/yr)
Present study	1992	165.1	4100	1.22	0.022	0.0038	IEA (4.0%/yr)

present NO_x emissions from aviation) used in this study cover the range of existing detailed model studies.

These are only a few of the uncertainties of aviation's impact on climate. The reader is referred to the IPCC Special Report 'Aviation and the Global Atmosphere' (IPCC, 1999), which discusses this in more detail. The uncertainties of the various model assumptions used in this study affect the quantitative results, while the qualitative result (that aviation emissions will have a growing share in climate change) seems to be insensitive to the model's uncertainties.

6. Conclusions

Using a combination of linear response models, we have estimated the impact of aviation on the atmospheric carbon dioxide concentration and on climate change in terms of global mean temperature and sea level. This study determined the global climatic impact for a wide range of scenarios of aviation fuel consumption and nitrogen oxides emissions, but cannot assess their validity. Nevertheless, the results for this set of scenarios can be used to discuss the consequences of alternative future trends in aviation fuel consumption and NO_x emissions.

Aviation fuel consumption contributes to the increase in atmospheric CO_2 concentration, which is computed to be on the order of 1.7% due to past aviation fuel consumption until 1995. Furthermore, it may increase to 2.9% and 3.2% in 2050 and 2100, respectively, for scenario *Fa1*, which is the reference case presently discussed in the IPCC Special Report 'Aviation and the Global Atmosphere'. Other scenarios have been set up which imply either smaller or even much larger increases in future CO_2 concentration due to aviation.

The response of the climate in terms of global mean surface temperature and mean sea level rise is slow. This is obvious from scenarios showing the response due to assumed sudden changes in the trends of future aviation emissions. The climate reacts to any trend changes in the emissions with a delay of several decades.

The transient response of temperature and sea level is about 35% to 75% of the equilibrium response for given radiative forcing. This is of importance when comparing studies with more complex climate models run with either constant or time-dependent radiative forcings.

The aviation impact due to CO_2 emissions on climate is small compared to all anthropogenic CO_2-induced climate changes, but the relative contribution of air traffic to global warming (in terms of global mean surface temperature) increases from a present-day fraction of about 0.8% to roughly 2.2% at the end of next century in the reference scenario. Other scenarios imply smaller or far larger responses.

The present study assumes that the radiative forcing due to ozone changes resulting from aviation NO_x emissions reacts more directly to changes in emission rates, while the thermal and sea level responses to O_3 changes also reflect the inertia of the Earth's system. In this parametric study, aviation-induced O_3 changes cause larger global temperature and sea level responses than CO_2 emissions of aviation in the 21st century. The O_3 impact is larger than the CO_2 impact by a factor between 1 and 10. As the forcing from aircraft-induced O_3 perturbations exhibits rather strong variations with latitude, regional climate changes may be considerably larger than global mean changes.

A reduction in aircraft NO_x emissions due to a low NO_x technology may reduce the aviation climate impact despite a small increase in aviation CO_2 emissions. This remains true even when the thermal equilibrium response to aircraft-induced O_3 increases induced by the NO_x emissions is low and near the lower bound of possible values considered in this study.

The present study suffers from many uncertainties. It relies on several recent studies which show that NO_x emissions from aviation cause an increase in O_3 in the upper troposphere, a positive radiative forcing, and, consequently, a temperature increase at the surface. Besides assessable uncertainties in past fuel consumption data (order 20%) and the carbon cycle model (order 20%), less known uncertainties result from the assumed thermal response model, the future scenarios, and, in particular, the assumed sensitivity of the surface temperature to NO_x emissions and O_3 changes.

Finally we would like to note that the present study used only CO_2 and NO_x emissions to study aviation impact on climate. We did not, for example, consider the effect of contrails. Due to the nature of our models, we only discuss global mean values and no regional responses.

Acknowledgements

The authors would like to thank Dr. S. Hasselmann and Dr. M. Heimann from the MPI für Meteorologie, Hamburg, for help in using the climate response models and for providing CO_2 concentration data according to the IPCC scenarios, respectively. We thank Dr. S. Baughcum from Boeing, Seattle, Dr. A. Vedantham from Environmental Defense Fund, Stockton College of New Jersey, and OECD Bonn for providing data on past and expected future aviation fuel consumption, and Prof. M. Prather from the University of California, Irvine, for helpful discussions. We also thank J. Freund for her assistance in preparing the plots.

References

Baughcum, S. L., Tritz, T. G., Henderson, S. C., and Pickett, D. C.: 1996a, *Scheduled Civil Aircraft Emission Inventories for 1992 – Database Development and Analysis*, NASA Contractor Report 4700.

Baughcum, S. L., Henderson, S. C., and Tritz, T. G.: 1996b, *Scheduled Civil Aircraft Emission Inventories for 1976 and 1984 – Database Development and Analysis*, NASA Contractor Report 4722.

Baughcum, S. L., Sutkus, D. J., and Henderson, S. C.: 1998, *Year 2015 Aircraft Emission Scenario for Scheduled Air Traffic*, NASA CR-1998-207638.

Brasseur, G. P., Cox, R. A., Hauglustaine, D., Isaksen, I., Lelieveld, J., Lister, D. H., Sausen, R., Schumann, U., Wahner, A., and Wiesen, P.: 1998, 'European Assessment of the Atmospheric Effects of Aircraft Emissions', *Atmos. Environ.* **32**, 2329–2418.

Cubasch, U., Hasselmann, K., Höck, H., Maier–Reimer, E., Mikolajewicz, U., Santer, B. D., and Sausen, R.: 1992, 'Time-Dependent Greenhouse Warming Computations with a Coupled Ocean-Atmosphere Model', *Clim. Dyn.* **8**, 55–69.

Dameris, M., Grewe, V., Köhler, I., Sausen, R., Brühl, C., Gross, J.-U., and Steil, B.: 1998, 'Impact of Aircraft NO_x-Emissions on Tropospheric and Stratospheric Ozone. Part II: 3-D Model Results', *Atmos. Environ.* **32**, 3185–3200.

Ehhalt, D. H. and Rohrer, F.: 1995, 'The Impact of Commercial Aircraft on Tropospheric Ozone', in Brandy, A. R. (ed.), *The Chemistry of the Atmosphere – Oxidants and Oxidation in the Earth's Atmosphere*, 7th BOC Priestley Conference, Lewisburg, Pennsylvania, 1994, The Royal Society of Chemistry, Special Publication No. 170, pp. 105–120.

Enting, I. G., Wigley, T. M. L., and Heimann, M.: 1994, *Future Emissions and Concentrations of Carbon Dioxide – Key Ocean/Atmosphere/Land Analyses*, CSIRO Division of Atmospheric Research Technical Paper No. 31, p. 120.

FESG: 1998, *Long Range Scenarios*, Report of the Forecasting and Economic Analysis Sub-Group (FESG), obtainable from Air Transport Bureau, ICAO, 999 University Street, Montreal, Quebec, H3C 5H7, Canada.

Friedl, R. (ed.): 1997, *Atmospheric Effects of Subsonic Aircraft – Interim Assessment Report of the Advanced Subsonic Technology Program*, NASA Reference Publication 1400, p. 143.

Gardener, R., Adams, K., Cook, T., Deidewig, F., Ernedal, S., Falk, R., Fleuti, E., Herms, E., Johnson, C. E., Lecht, M., Lee, D. S., Leech, M., Lister, D., Massé, B., Metcalfe, M., Newton, P., Schmitt, A., Vandenbergh, C., and van Drimmelen, R.: 1997, 'The ANCAT/EC Global Inventory of NO_x Emissions from Aircraft', *Atmos. Environ.* **31**, 1751–1766.

Gardener, R. M., Adams, J. K., Cook, T., Larson, L. G., Falk, R. S., Fleuti, E., Förtsch, W., Lecht, M., Lee, D. S., Leech, M. V., Lister, D. H., Massé, B., Morris, K., Newton, P. J., Owen, A., Parker, E., Schmitt, A., ten Have, H., and Vandenberghe, C.: 1998, *ANCAT/EC2 Global Aircraft Emissions Inventories for 1991/92 and 2015*, Eur No. 18179, ISBN 92-828-2914-6.

Grewe, V., Dameris, M., Hein, R., Koehler, I., and Sausen, R.: 1999, 'Impact of Future Subsonic Aircraft NO_x Emissions on the Atmospheric Composition', *Geophys. Res. Lett.* **26**, 47–50.

Grooß, J.-U., Brühl, C., and Peter, T.: 1998, 'Impact of Aircraft NO_x-Emissions on Tropospheric and Stratospheric Ozone. Part I: Chemistry and 2-D Model Results', *Atmos. Environ.* **32**, 3173–3184.

Hansen, J., Sato, M., and Ruedy, R.: 1997, 'Radiative Forcing and Climate Response', *J. Geophys. Res.* **102**, 6831–6864.

Hasselmann, K., Sausen, R., Maier-Reimer, E., and Voss, R.: 1993, 'On the Cold Start Problem in Transient Simulations with Coupled Atmosphere-Ocean Models', *Clim. Dyn.* **9**, 53–61.

Hasselmann, K., Hasselmann, S., Giering, R., Ocana, V., and von Storch, H.: 1997, 'Sensitivity Study of Optimal CO_2 Emission Paths Using a Simplified Structural Integrated Assessment Model (SIAM)', *Clim. Change* **37**, 345–386.

Hauglustaine, D. A., Granier, C., Brasseur, G. P., and Megie, G.: 1994, 'Impact of Present Aircraft Emissions of Nitrogen Oxides on Tropospheric Ozone and Climate Forcing', *Geophys. Res. Lett.* **21**, 2031–2034.

IEA: 1991, *Oil and Gas Information 1988–1990. Table 4: World Demand by Main Product Groups, World, Aviation Fuels*, IEA/OECD, 2, rue Andre-Pascal, 75775 Paris Cedex 16, France.

IPCC: 1990, Houghton, J. T., Jenkins, G. J., and Ephraums, J. J. (eds.), *Climate Change – The IPCC Scientific Assessment*, Cambridge University Press, Cambridge, U.K., p. 365.

IPCC: 1992, Houghton, J. H., Callander, B. A., and Varney, S. K. (eds.), *Climate Change 1992 – The Supplementary Report to the IPCC Scientific Assessment*, Cambridge University Press, Cambridge, U.K., p. 200.

IPCC: 1995, Houghton, J. T., Meira Filho, L. G., Bruce, J., Lee, Hoesung, Callander, B. A., Harris, N., and Maskell, K. (eds.), *Climate Change 1994 – Radiative Forcing of Climate Change and an Evaluation of the IPCC IS92 Emission Scenarios*, Cambridge University Press, Cambridge, U.K., p. 339.

IPCC: 1996, Houghton, J. H., Meira Filho, L. G., Callander, B. A., Harris, N., Kattenberg, A., and Maskell, K. (eds.), *Climate Change 1995 – The Science of Climate Change*, Cambridge University Press, Cambridge, U.K., p. 572.

IPCC: 1999, Penner, J. E., Lister, D. H., Griggs, D. J., Dokken, D. J., and McFarland, M. (eds.), *Aviation and the Global Atmosphere – A Special Report of IPCC Working Groups I and III*, Cambridge University Press, Cambridge, U.K., p. 373.

Joos, F., Bruno, M., Fink, R., Siegenthaler, U., Stocker, T. F., Le Quere, C., and Sarmiento, J. L.: 1996, 'An Efficient and Accurate Representation of Complex Oceanic and Biospheric Models of Anthropogenic Carbon Uptake', *Tellus* **48B**, 397–417.

Maier-Reimer, E.: 1987, 'The Biological Pump in the Greenhouse', *Global Plan. Clim. Change* **8**, 13–15.

Maier-Reimer, E. and Hasselmann, K.: 1987, 'Transport and Storage of CO_2 in the Ocean – An Inorganic Ocean-Circulation Carbon Cycle Model', *Clim. Dyn.* **2**, 63–90.

Masood, E.: 1997, 'Asian Economies Lead Increase in Carbon Dioxide Emissions', *Nature* **388**, 213.

Nüsser, H.-G. and Schmitt, A.: 1990, 'The Global Distribution of Air Traffic at High Altitudes, Related Fuel Consumption and Trends', in Schumann, U. (ed.), *Air Traffic and the Environment – Background, Tendencies and Potential Global Atmospheric Effects*, Lecture Notes in Engineering, Springer-Verlag, Berlin, Heidelberg, pp. 1–11.

Ponater, M., Brinkop, S., Sausen, R., and Schumann, U.: 1996, 'Simulating the Global Atmospheric Response to Aircraft Water Vapour Emissions and Contrails – A First Approach Using a GCM', *Ann. Geophys.* **14**, 941–960.

Ponater, M., Sausen, R., Feneberg, B., and Roeckner, E.: 1999, 'Equilibrium Climate Response to Aircraft Induced Ozone Changes', *Clim. Dyn.*, in press. Also available as Report No. 103, DLR – Institut für Physik der Atmosphäre, Oberpfaffenhofen, Germany, ISSN 0943-4771, p. 26.

Rind, D. and Lonergan, P.: 1995, 'Modeled Impacts of Stratospheric Ozone and Water Vapor Perturbations with Implications for High-Speed Civil Transport Aircraft', *J. Geophys. Res.* **100**, 7381–7396.

Rind, D., Lonergan, P., and Shah, K.: 1996, 'Climatic Effect of Water Vapor Release in the Upper Troposphere', *J. Geophys. Res.* **101**, 29395–29406.

Sausen, R., Feneberg, B., and Ponater, M.: 1997, 'Climatic Impact of Aircraft Induced Ozone Changes', *Geophys. Res. Lett.* **24**, 1203–1206.

Schmitt, A. and Brunner, B.: 1997, *Emissions from Aviation and Their Development over Time*, DLR–Mitteilung, 97-04, DLR Köln, pp. 37–52.

Schumann, U.: 1997, 'The Impact of Nitrogen Oxides Emissions from Aircraft upon the Atmosphere at Flight Altitudes, Results from the AERONOX Project', *Atmos. Environ.* **31**, 1723–1733.

Siegenthaler, U. and Joos, F.: 1992, 'Use of a Simple Model for Studying Oceanic Tracer Distributions and the Global Carbon Cycle', *Tellus* **44B**, 186–207.

Vedantham, A. and Oppenheimer, M.: 1998, 'Long-Term Scenarios for Aviation: Demand and Emissions of CO_2 and NO_x', *Energy Policy* **8**, 625–641.

(Received 25 March 1998; in revised form 23 March 1999)